

Electronic Supplementary Information

Self-assembly of octanuclear Ln(III)-based clusters for large magnetocaloric effect and highly efficient conversion of CO₂

Wen-Min Wang,^{a,c} Xiao-Yan Xin,^a Na Qiao,^a Zhi-Lei Wu^{*c,d} Ling Li^b and Ji-Yong Zou^{* b,e}

Experimental section

Materials and methods

Ln(III) nitrate hexahydrate ($\text{Ln}(\text{NO}_3)_2 \cdot 6\text{H}_2\text{O}$, Ln = Gd, Dy, and Ho), acetylacetone, ammonium hydroxide (28.0-30.0%) 5-hydroxymethylfurfural, 2-picolinylhydrazide and salicyl hydrazide were obtained from Energy Chemical Co. Ltd. The solvents methanol, ethanol and dichloromethane were received from Beijing Chemical Reagent Company. All of these chemical reactants and reagents were directly used without further purification. The two polydentate Schiff-base ligand (HL) were synthesized as the previously similar method.¹ The β -diketone salts $\text{Ln}(\text{acac})_3 \cdot 2\text{H}_2\text{O}$ (Ln(III) = Gd, Dy, and Ho) were synthesized according to the method reported in the literature.²

The elemental analysis (C, H, and N) of Schiff-base ligand (HL) and clusters **1-3** were measured at the Institute of Elemental Organic Chemistry, Nankai University. The infrared (IR) spectra of Schiff-base ligands (HL) and clusters **1-3** were obtained using a Bruker Tensor 27 spectrophotometer. Powder X-ray diffraction (PXRD) of clusters **1-3** were measured on Ultima IV (Rigaku) with Cu K α radiation. Thermogravimetric analysis (TGA) of clusters **1-3** were performed on a TG 209 apparatus (Netzsch) under an air atmosphere. The UV-vis absorbance spectra of

^a College of Chemistry and Materials, Taiyuan Normal University, Jinzhong, 030619, China

^b Institute of Applied Chemistry, Jiangxi Academy of Sciences, Nanchang 330096, China.

^c Department of Chemistry, Tianjin University, Tianjin, 300072, China

^d College of Chemistry and Environmental Science, Hebei University, Baoding, 071002, China

^e Key Laboratory of Advanced Energy Materials Chemistry (Ministry of Education), Nankai University, Tianjin, 300071, PR China

*Corresponding Authors E-mail: zoujiyong@jxas.ac.cn, wuzhilei03@163.com

Schiff-base ligands (HL) and clusters **1-3** were performed measured on a TU-1950 UV-vis spectrophotometer. The fluorescence emission spectra of cluster **1** was recorded on a *F*-320 fluorospectro photometer. X-ray photoelectron spectroscopy (XPS) was performed on a Kratos Axis Ultra DLD multi-technique X-ray spectrometer. ¹HNMR spectra were performed on a 400 MHz Bruker 400 spectrometer in CDCl₃. Inductively coupled plasma (ICP) measurements were performed on an ICP-9000(N + M). The Dc and Ac magnetic properties data of clusters **1-3** were performed on polycrystalline samples using a Quantum Design MPMS (SQUID)-XL magnetometer and PPMS-9T system.

Catalytic reactions of CO₂ and epoxides

20 mg cluster **1**, TBAB (2.5 mmol %), epoxides substrate (2.0 mmol) and excess CO₂ were sealed in a 50 mL Schlenk tube, and stirred at 25-90 °C for 10 h. The corresponding yield was analyzed by ¹HNMR with 1,3,5-trimethoxybenzene as an internal standard.

Catalytic recyclable experiments of CO₂ and epoxides

After the catalytic reaction, the catalyst **1** was isolated by centrifugation, washed with fresh CH₂Cl₂ for three times and dried naturally. The recovered catalyst was used for the next cycle.

Tables S1 Selected bond lengths (Å) and angles (°) for cluster **1**^a

Bond lengths			
Gd(4)-O(16)#1	2.194(4)	Gd(4)-O(15)	2.360(4)
Gd(4)-O(3)	2.410(4)	Gd(4)-O(12)	2.290(4)
Gd(4)-O(9)	2.304(5)	Gd(4)-O(8)	2.335(5)
Gd(4)-O(14)#1	2.389(4)	Gd(2)-Gd(1)#1	3.7355(5)
Gd(2)-O(16)#1	2.214(4)	Gd(2)-O(15)#1	2.380(4)
Gd(2)-O(3)	2.406(4)	Gd(2)-O(4)	2.270(4)
Gd(2)-O(5)	2.389(4)	Gd(2)-O(13)	2.314(5)
Gd(2)-O(14)	2.308(5)	Gd(1)-O(16)	2.249(4)
Gd(1)-O(15)	2.385(4)	Gd(1)-O(3)	2.684(4)
Gd(1)-O(10)	2.302(4)	Gd(1)-O(11)	2.455(5)
Gd(1)-O(2)	2.680(4)	Gd(1)-O(14)	2.368(4)
Gd(1)-O(1)	2.396(4)	Gd(3)-O(16)#1	2.343(4)
Gd(3)-O(13)	2.269(4)	Gd(3)-O(12)	2.273(4)
Gd(3)-O(7)	2.354(5)	Gd(3)-O(11)#1	2.690(4)

Gd(3)-O(6)	2.339(5)	Gd(3)-O(1)#1	2.329(5)
Gd(1)-N(3)	2.704(6)	Gd(3)-N(1)#1	2.677(6)
Bond angles			
O(16)#1-Gd(4)-O(15)	108.81(15)	O(16)#1-Gd(4)-O(3)	72.79(15)
O(16)#1-Gd(4)-O(12)	74.56(15)	O(16)#1-Gd(4)-O(9)	115.55(16)
O(16)#1-Gd(4)-O(8)	163.01(17)	O(16)#1-Gd(4)-O(14)#1	73.14(16)
O(15)-Gd(4)-O(3)	71.57(15)	O(15)-Gd(4)-O(14)#1	74.33(14)
O(12)-Gd(4)-O(15)	157.85(15)	O(12)-Gd(4)-O(3)	89.30(16)
O(12)-Gd(4)-O(9)	81.22(17)	O(12)-Gd(4)-O(8)	94.48(16)
O(12)-Gd(4)-O(14)#1	126.36(15)	O(9)-Gd(4)-O(15)	114.80(17)
O(9)-Gd(4)-O(3)	164.73(16)	O(9)-Gd(4)-O(8)	74.47(17)
O(9)-Gd(4)-O(14)#1	75.72(16)	O(8)-Gd(4)-O(15)	76.54(15)
O(8)-Gd(4)-O(3)	94.51(16)	O(8)-Gd(4)-O(14)#1	123.67(17)
O(14)#1-Gd(4)-O(3)	119.52(14)	O(16)#1-Gd(2)-O(15)#1	71.54(15)
O(16)#1-Gd(2)-O(3)	72.54(15)	O(16)#1-Gd(2)-O(4)	76.59(16)
O(16)#1-Gd(2)-O(5)	131.01(16)	O(16)#1-Gd(2)-O(13)	148.99(16)
O(16)#1-Gd(2)-O(14)	112.42(15)	O(15)#1-Gd(2)-O(3)	117.28(15)
O(15)#1-Gd(2)-O(14)	73.96(14)	O(13)-Gd(2)-O(15)#1	118.60(14)
O(13)-Gd(2)-O(3)	100.32(15)	O(13)-Gd(2)-O(5)	92.55(17)
O(13)-Gd(2)-O(4)	85.66(16)	O(13)-Gd(2)-O(14)	167.03(15)
O(5)-Gd(2)-O(15)#1	72.74(17)	O(5)-Gd(2)-O(3)	155.67(15)
O(5)-Gd(2)-O(4)	74.22(17)	O(5)-Gd(2)-O(14)	88.17(15)
O(4)-Gd(2)-O(15)#1	139.39(15)	O(4)-Gd(2)-O(3)	86.17(16)
O(4)-Gd(2)-O(14)	82.07(16)	O(14)-Gd(2)-O(3)	74.74(14)
O(16)-Gd(1)-O(15)	70.88(14)	O(16)-Gd(1)-O(3)	107.47(13)
O(16)-Gd(1)-O(10)	139.67(17)	O(16)-Gd(1)-O(11)	70.44(15)
O(16)-Gd(1)-O(2)	150.98(15)	O(16)-Gd(1)-O(14)	72.59(16)
O(16)-Gd(1)-O(1)	68.96(15)	O(15)-Gd(1)-O(3)	66.47(14)
O(15)-Gd(1)-O(11)	72.66(14)	O(15)-Gd(1)-O(2)	115.22(14)
O(15)-Gd(1)-O(1)	129.78(15)	O(10)-Gd(1)-O(15)	83.81(16)
O(10)-Gd(1)-O(3)	89.40(14)	O(10)-Gd(1)-O(11)	72.32(16)
O(10)-Gd(1)-O(2)	68.40(16)	O(10)-Gd(1)-O(14)	147.16(17)
O(10)-Gd(1)-O(1)	109.04(16)	O(11)-Gd(1)-O(3)	136.72(14)
O(11)-Gd(1)-O(2)	138.40(14)	O(2)-Gd(1)-O(3)	56.48(13)
O(14)-Gd(1)-O(15)	109.15(14)	O(14)-Gd(1)-O(3)	70.02(14)
O(14)-Gd(1)-O(11)	139.83(15)	O(14)-Gd(1)-O(2)	78.84(14)
O(14)-Gd(1)-O(1)	86.16(15)	O(1)-Gd(1)-O(3)	155.51(15)
O(1)-Gd(1)-O(11)	66.39(15)	O(1)-Gd(1)-O(2)	114.61(14)
O(16)#1-Gd(3)-O(7)	138.34(15)	O(16)#1-Gd(3)-O(11)#1	64.95(13)
O(13)-Gd(3)-O(16)#1	74.09(15)	O(13)-Gd(3)-O(12)	94.88(16)
O(13)-Gd(3)-O(7)	98.79(17)	O(13)-Gd(3)-O(11)#1	78.14(14)
O(13)-Gd(3)-O(6)	85.24(16)	O(13)-Gd(3)-O(1)#1	134.70(15)
O(12)-Gd(3)-O(16)#1	72.11(14)	O(12)-Gd(3)-O(7)	149.16(15)
O(12)-Gd(3)-O(11)#1	136.81(14)	O(12)-Gd(3)-O(6)	81.72(16)

O(12)-Gd(3)-O(1)#1	97.19(17)	O(7)-Gd(3)-O(11)#1	73.40(14)
O(6)-Gd(3)-O(16)#1	144.69(15)	O(6)-Gd(3)-O(7)	72.09(17)
O(6)-Gd(3)-O(11)#1	138.62(16)	O(1)#1-Gd(3)-O(16)#1	68.60(15)
O(1)#1-Gd(3)-O(7)	92.62(17)	O(1)#1-Gd(3)-O(11)#1	63.44(15)
O(1)#1-Gd(3)-O(6)	139.67(16)		

^a Symmetry transformation used to generate equivalent atoms: #1 -x+2, -y, -z+1

Tables S2 Selected bond lengths (\AA) and angles ($^{\circ}$) for cluster **2^a**

Bond lengths			
Dy(2)-O(14)	2.210(7)	Dy(2)-O(15)	2.375(8)
Dy(2)-O(16)#1	2.349(7)	Dy(2)-O(12)	2.275(7)
Dy(2)-O(7)	2.334(8)	Dy(2)-O(6)	2.306(8)
Dy(2)-O(3)#1	2.406(7)	Dy(1)-O(14)	2.359(7)
Dy(1)-O(13)	2.282(8)	Dy(1)-O(12)	2.286(7)
Dy(1)-O(4)	2.340(7)	Dy(1)-O(5)	2.317(7)
Dy(1)-O(1)	2.327(8)	Dy(1)-O(10)	2.697(8)
Dy(4)-O(14)#1	2.198(7)	Dy(4)-O(15)	2.394(7)
Dy(4)-O(16)#1	2.381(8)	Dy(4)-O(13)#1	2.267(7)
Dy(4)-O(8)	2.313(8)	Dy(4)-O(9)	2.310(8)
Dy(4)-O(3)	2.417(7)	Dy(3)-O(14)	2.235(7)
Dy(3)-O(15)	2.353(8)	Dy(3)-O(16)	2.373(8)
Dy(3)-O(11)	2.291(7)	Dy(3)-O(3)	2.663(7)
Dy(3)-O(2)	2.693(8)	Dy(3)-O(1)	2.395(8)
Dy(3)-O(10)	2.455(8)	Dy(1)-N(1)	2.708(10)
Dy(3)-N(3)	2.723(11)		
Bond angles			
O(14)-Dy(2)-O(15)	72.5(3)	O(14)-Dy(2)-O(16)#1	108.0(3)
O(14)-Dy(2)-O(12)	75.4(3)	O(14)-Dy(2)-O(7)	163.0(3)
O(14)-Dy(2)-O(6)	116.4(3)	O(14)-Dy(2)-O(3)#1	72.7(3)
O(15)-Dy(2)-O(3)#1	119.2(3)	O(16)#1-Dy(2)-O(15)	74.5(3)
O(16)#1-Dy(2)-O(3)#1	71.2(3)	O(12)-Dy(2)-O(15)	126.2(3)
O(12)-Dy(2)-O(16)#1	157.9(3)	O(12)-Dy(2)-O(7)	94.0(3)
O(12)-Dy(2)-O(6)	81.4(3)	O(12)-Dy(2)-O(3)#1	89.8(3)
O(7)-Dy(2)-O(15)	124.2(3)	O(7)-Dy(2)-O(16)#1	76.9(3)
O(7)-Dy(2)-O(3)#1	94.3(3)	O(6)-Dy(2)-O(15)	75.8(3)
O(6)-Dy(2)-O(16)#1	114.4(3)	O(6)-Dy(2)-O(7)	74.1(3)
O(6)-Dy(2)-O(3)#1	164.8(3)	O(14)-Dy(1)-O(10)	64.3(2)
O(13)-Dy(1)-O(14)	73.8(3)	O(13)-Dy(1)-O(12)	95.0(3)
O(13)-Dy(1)-O(4)	99.1(3)	O(13)-Dy(1)-O(5)	85.5(3)
O(13)-Dy(1)-O(1)	134.6(3)	O(13)-Dy(1)-O(10)	77.9(3)
O(12)-Dy(1)-O(14)	72.4(2)	O(12)-Dy(1)-O(4)	149.4(3)
O(12)-Dy(1)-O(5)	82.0(3)	O(12)-Dy(1)-O(1)	96.8(3)
O(12)-Dy(1)-O(10)	136.4(2)	O(4)-Dy(1)-O(14)	137.8(3)
O(4)-Dy(1)-O(10)	73.5(2)	O(5)-Dy(1)-O(14)	145.0(2)

O(5)-Dy(1)-O(4)	72.3(3)	O(5)-Dy(1)-O(1)	139.5(3)
O(5)-Dy(1)-O(10)	138.8(3)	O(1)-Dy(1)-O(14)	68.5(3)
O(1)-Dy(1)-O(4)	92.5(3)	O(1)-Dy(1)-O(10)	63.6(3)
O(14)#1-Dy(4)-O(15)	111.6(3)	O(14)#1-Dy(4)-O(16)#1	70.9(3)
O(14)#1-Dy(4)-O(13)#1	77.2(3)	O(14)#1-Dy(4)-O(8)	130.2(3)
O(14)#1-Dy(4)-O(9)	149.7(3)	O(14)#1-Dy(4)-O(3)	72.7(2)
O(15)-Dy(4)-O(3)	74.4(3)	O(16)#1-Dy(4)-O(15)	73.5(2)
O(16)#1-Dy(4)-O(3)	116.8(3)	O(13)#1-Dy(4)-O(15)	167.1(3)
O(13)#1-Dy(4)-O(16)#1	119.0(2)	O(13)#1-Dy(4)-O(8)	92.3(3)
O(13)#1-Dy(4)-O(9)	85.2(3)	O(13)#1-Dy(4)-O(3)	100.4(3)
O(8)-Dy(4)-O(15)	88.9(3)	O(8)-Dy(4)-O(16)#1	72.7(3)
O(8)-Dy(4)-O(3)	156.3(3)	O(9)-Dy(4)-O(15)	82.8(3)
O(9)-Dy(4)-O(16)#1	139.4(3)	O(9)-Dy(4)-O(8)	74.3(3)
O(9)-Dy(4)-O(3)	86.7(3)	O(14)-Dy(3)-O(15)	72.5(3)
O(14)-Dy(3)-O(16)	70.4(3)	O(14)-Dy(3)-O(11)	139.8(3)
O(14)-Dy(3)-O(3)	107.5(2)	O(14)-Dy(3)-O(2)	151.0(2)
O(14)-Dy(3)-O(1)	69.4(3)	O(14)-Dy(3)-O(10)	70.2(2)
O(15)-Dy(3)-O(16)	109.1(3)	O(15)-Dy(3)-O(3)	70.6(2)
O(15)-Dy(3)-O(2)	78.9(3)	O(15)-Dy(3)-O(1)	85.7(3)
O(15)-Dy(3)-O(10)	139.5(3)	O(16)-Dy(3)-O(3)	66.4(2)
O(16)-Dy(3)-O(2)	116.0(2)	O(16)-Dy(3)-O(1)	129.9(3)
O(16)-Dy(3)-O(10)	72.5(2)	O(11)-Dy(3)-O(15)	147.2(3)
O(11)-Dy(3)-O(16)	84.6(3)	O(11)-Dy(3)-O(3)	89.4(2)
O(11)-Dy(3)-O(2)	68.4(3)	O(11)-Dy(3)-O(1)	108.6(3)
O(11)-Dy(3)-O(10)	72.5(3)	O(3)-Dy(3)-O(2)	57.1(2)
O(1)-Dy(3)-O(3)	155.6(3)	O(1)-Dy(3)-O(2)	113.7(3)
O(1)-Dy(3)-O(10)	66.7(3)	O(10)-Dy(3)-O(3)	136.4(2)
O(10)-Dy(3)-O(2)	138.5(2)		

^a Symmetry transformations used to generate equivalent atoms: #1 -x+1, -y+1, -z

Tables S3 Selected bond lengths (Å) and angles (°) for cluster 3^a

Bond lengths			
Ho(1)-O(15)	2.180(6)	Ho(1)-O(16)#1	2.341(5)
Ho(1)-O(14)	2.377(5)	Ho(1)-O(12)	2.268(5)
Ho(1)-O(5)	2.332(7)	Ho(1)-O(4)	2.305(6)
Ho(1)-O(1)#1	2.396(5)	Ho(3)-O(15)	2.238(5)
Ho(3)-O(16)	2.379(5)	Ho(3)-O(14)	2.360(6)
Ho(3)-O(8)	2.296(6)	Ho(3)-O(9)	2.454(6)
Ho(3)-O(1)	2.696(5)	Ho(3)-O(2)	2.692(6)
Ho(3)-O(3)	2.385(6)	Ho(4)-O(15)#1	2.212(5)
Ho(4)-O(16)#1	2.376(6)	Ho(4)-O(14)	2.376(5)
Ho(4)-O(13)	2.258(5)	Ho(4)-O(1)	2.387(6)
Ho(4)-O(7)	2.303(7)	Ho(4)-O(6)	2.310(6)
Ho(2)-O(15)	2.322(5)	Ho(2)-O(13)#1	2.265(6)

Ho(2)-O(12)	2.274(6)	Ho(2)-O(10)	2.338(5)
Ho(2)-O(9)	2.695(6)	Ho(2)-O(11)	2.324(6)
Ho(2)-O(3)	2.324(6)	Ho(3)-N(1)	2.692(7)
Ho(2)-N(3)	2.664(7)		
Bond angles			
O(15)-Ho(1)-Ho(3)	34.44(14)	O(15)-Ho(1)-Ho(4)	89.30(14)
O(15)-Ho(1)-Ho(4)#1	33.46(13)	O(15)-Ho(1)-Ho(2)	38.69(13)
O(15)-Ho(1)-O(16)#1	109.3(2)	O(15)-Ho(1)-O(14)	73.3(2)
O(15)-Ho(1)-O(12)	74.8(2)	O(15)-Ho(1)-O(5)	163.1(2)
O(15)-Ho(1)-O(4)	114.9(2)	O(15)-Ho(1)-O(1)#1	72.97(19)
O(16)#1-Ho(1)-Ho(3)	96.29(14)	O(16)#1-Ho(1)-Ho(4)	37.21(13)
O(16)#1-Ho(1)-Ho(4)#1	90.05(14)	O(16)#1-Ho(1)-Ho(2)	147.35(15)
O(16)#1-Ho(1)-O(14)	74.48(18)	O(16)#1-Ho(1)-O(1)#1	71.89(18)
O(14)-Ho(1)-O(1)#1	119.9(2)	O(12)-Ho(1)-O(16)#1	157.6(2)
O(12)-Ho(1)-O(14)	126.70(18)	O(12)-Ho(1)-O(5)	94.0(2)
O(12)-Ho(1)-O(4)	81.1(2)	O(12)-Ho(1)-O(1)#1	89.1(2)
O(5)-Ho(1)-O(16)#1	76.4(2)	O(5)-Ho(1)-O(14)	123.5(2)
O(5)-Ho(1)-O(1)#1	94.6(2)	O(4)-Ho(1)-O(16)#1	114.8(2)
O(4)-Ho(1)-O(14)	75.2(2)	O(4)-Ho(1)-O(5)	74.8(2)
O(4)-Ho(1)-O(1)#1	164.9(2)	O(15)-Ho(3)-O(16)	71.2(2)
O(15)-Ho(3)-O(14)	72.66(19)	O(15)-Ho(3)-O(8)	140.4(2)
O(15)-Ho(3)-O(9)	70.47(19)	O(15)-Ho(3)-O(1)	107.54(17)
O(15)-Ho(3)-O(2)	150.88(19)	O(15)-Ho(3)-O(3)	68.97(18)
O(16)-Ho(3)-O(9)	72.52(18)	O(16)-Ho(3)-O(1)	66.13(17)
O(16)-Ho(3)-O(2)	114.85(18)	O(16)-Ho(3)-O(3)	130.29(19)
O(14)-Ho(3)-O(16)	108.84(18)	O(14)-Ho(3)-O(9)	140.2(2)
O(14)-Ho(3)-O(1)	69.79(18)	O(14)-Ho(3)-O(2)	78.65(18)
O(14)-Ho(3)-O(3)	86.29(19)	O(8)-Ho(3)-O(16)	84.1(2)
O(8)-Ho(3)-O(14)	146.3(2)	O(8)-Ho(3)-O(9)	72.9(2)
O(8)-Ho(3)-O(1)	88.86(18)	O(8)-Ho(3)-O(2)	67.7(2)
O(8)-Ho(3)-O(3)	109.4(2)	O(9)-Ho(3)-O(1)	136.23(19)
O(9)-Ho(3)-O(2)	138.49(18)	O(2)-Ho(3)-O(1)	56.39(15)
O(3)-Ho(3)-O(9)	67.0(2)	O(3)-Ho(3)-O(1)	155.4(2)
O(3)-Ho(3)-O(2)	114.49(18)	O(15)#1-Ho(4)-O(16)#1	71.7(2)
O(15)#1-Ho(4)-O(14)	112.80(19)	O(15)#1-Ho(4)-O(13)	76.4(2)
O(15)#1-Ho(4)-O(1)	72.61(18)	O(15)#1-Ho(4)-O(7)	130.3(2)
O(15)#1-Ho(4)-O(6)	148.6(2)	O(16)#1-Ho(4)-O(1)	117.52(19)
O(14)-Ho(4)-O(16)#1	73.87(17)	O(14)-Ho(4)-O(1)	75.19(19)
O(13)-Ho(4)-O(16)#1	118.77(18)	O(13)-Ho(4)-O(14)	166.92(19)
O(13)-Ho(4)-O(1)	99.9(2)	O(13)-Ho(4)-O(7)	92.1(2)
O(13)-Ho(4)-O(6)	85.3(2)	O(7)-Ho(4)-O(16)#1	72.6(2)
O(7)-Ho(4)-O(14)	88.6(2)	O(7)-Ho(4)-O(1)	156.5(2)
O(7)-Ho(4)-O(6)	74.8(2)	O(6)-Ho(4)-O(16)#1	139.7(2)
O(6)-Ho(4)-O(14)	82.29(19)	O(6)-Ho(4)-O(1)	86.0(2)

O(15)-Ho(2)-O(10)	137.7(2)	O(15)-Ho(2)-O(9)	64.98(17)
O(15)-Ho(2)-O(11)	144.86(19)	O(15)-Ho(2)-O(3)	68.67(18)
O(13) ^{#1} -Ho(2)-O(15)	74.08(19)	O(13) ^{#1} -Ho(2)-O(12)	94.9(2)
O(13) ^{#1} -Ho(2)-O(10)	99.1(2)	O(13) ^{#1} -Ho(2)-O(9)	77.69(19)
O(13) ^{#1} -Ho(2)-O(11)	85.0(2)	O(13) ^{#1} -Ho(2)-O(3)	134.7(2)
O(12)-Ho(2)-O(15)	72.00(19)	O(12)-Ho(2)-O(10)	149.7(2)
O(12)-Ho(2)-O(9)	136.77(18)	O(12)-Ho(2)-O(11)	82.2(2)
O(12)-Ho(2)-O(3)	97.2(2)	O(10)-Ho(2)-O(9)	72.80(19)
O(11)-Ho(2)-O(10)	72.5(2)	O(11)-Ho(2)-O(9)	137.9(2)
O(11)-Ho(2)-O(3)	139.8(2)	O(3)-Ho(2)-O(10)	91.8(2)
O(3)-Ho(2)-O(9)	63.9(2)		

^a Symmetry transformation used to generate equivalent atoms: #1 -x+1, -y+1, -z

Table S4 The Gd^{III} geometry analysis by SHAPE 2.0 for cluster 1.

Cluster 2	C _{4v} JCCU	C _{4v} CCU	C _{4v} CSAPR	C _{2v} HH	C _s MFF
Gd1 ^{III}	5.690	4.726	6.554	4.427	5.559
	D_{4d}SAPR	D_{2d}TDD	C_{2v}JBTPR	C_{2v}BTPR	D_{2d}JSD
Gd3 ^{III}	3.549	1.143	3.144	3.107	2.560
	D_{5h}PBPY	C_{3v}CO	C_{2v}TPR	D_{5h}JPBPY	C_{3v}JETPY
Gd2 ^{III}	5.156	1.917	0.985	9.075	19.326
	C_{6v}HPY	D_{5h}PBPY	C_{3v}CO	C_{2v}TPR	D_{5h}JPBPY
Gd4 ^{III}	2.647	1.463	2.494	1.556	3.767

JCCU-9 = Capped cube J8; **CCU-9** = Spherical-relaxed capped cube; **CSAPR-9** = Spherical capped square antiprism; **HH-9** = Hula-hoop; **MFF-9** = Muffin.

SAPR-8 = Square antiprism; **TDD-8** = Triangular dodecahedron; **JBTPR-8** = Biaugmented trigonal prism J50; **BTPR-8** = Biaugmented trigonal prism; **JSD-8** = Snub diphenoid J84.

HPY-7 = Hexagonal pyramid; **PBPY-7** = Pentagonal bipyramid; **COC-7** = Capped octahedron; **TPR-7** = Capped trigonal prism; **JPBPY-7** = Johnson pentagonal bipyramid J13; **JETPY-7** = Johnson elongated triangular pyramid J7.

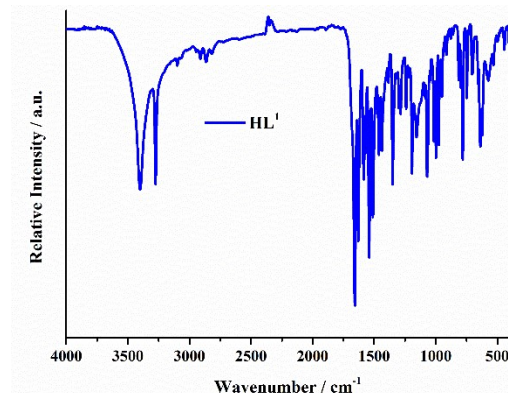


Fig. S1 The IR spectra of HL.

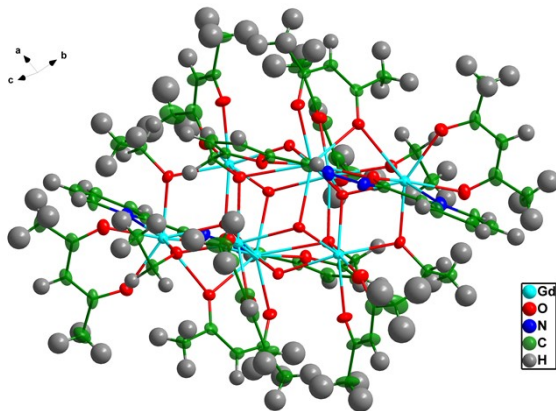


Fig. S2 Molecular structure of **1** with 50% probability ellipsoids (Symmetry code #1: -x+2, -y, -z+1, atoms in **1** are not labeled due to the large structure and lots of atoms for **1**).

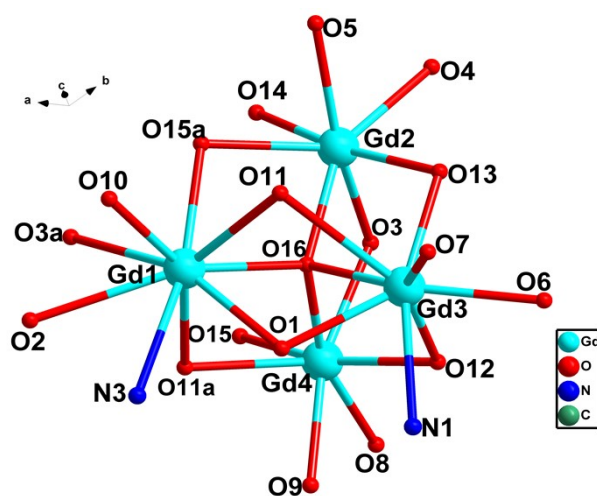
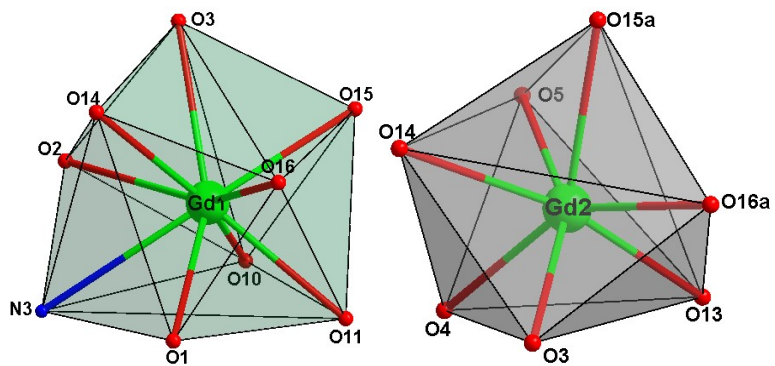


Fig. S3 The coordinate atom labels of central Gd(III) ions in cluster 1.



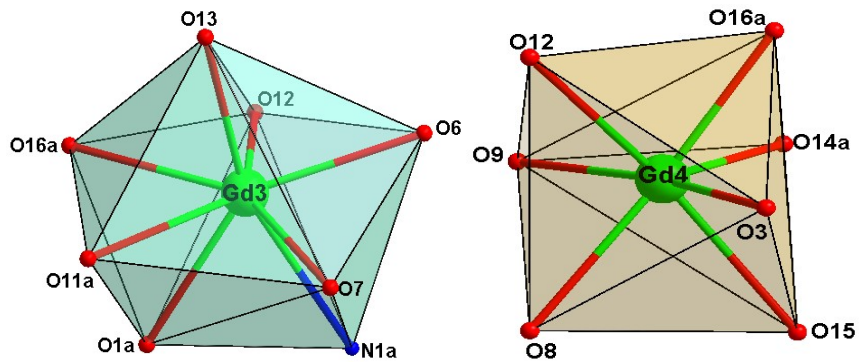


Fig. S4 The coordination polyhedron of central Gd(III) ions in cluster **1**.

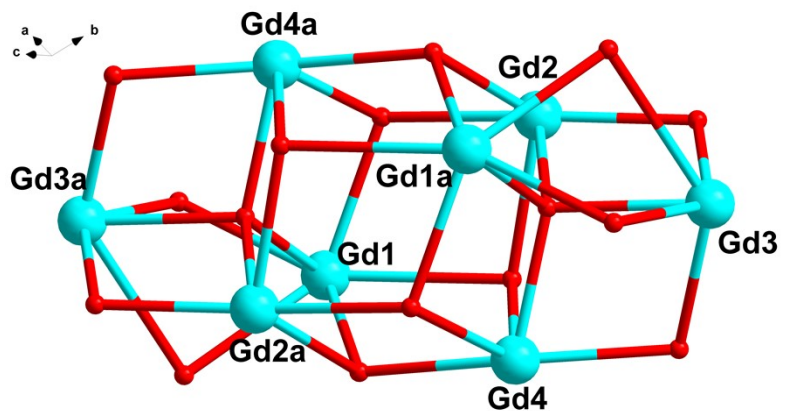


Fig. S5 The Gd₈ core bridged by eighteen μ_2 -O atoms, six μ_3 -O atoms and two μ_4 -O atoms in **1**.

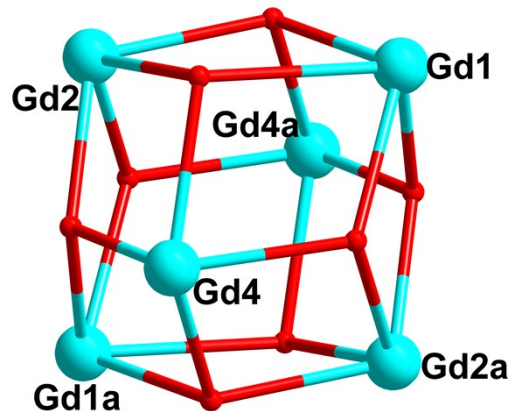


Fig. S6 The Gd₆ cage in cluster **1**.

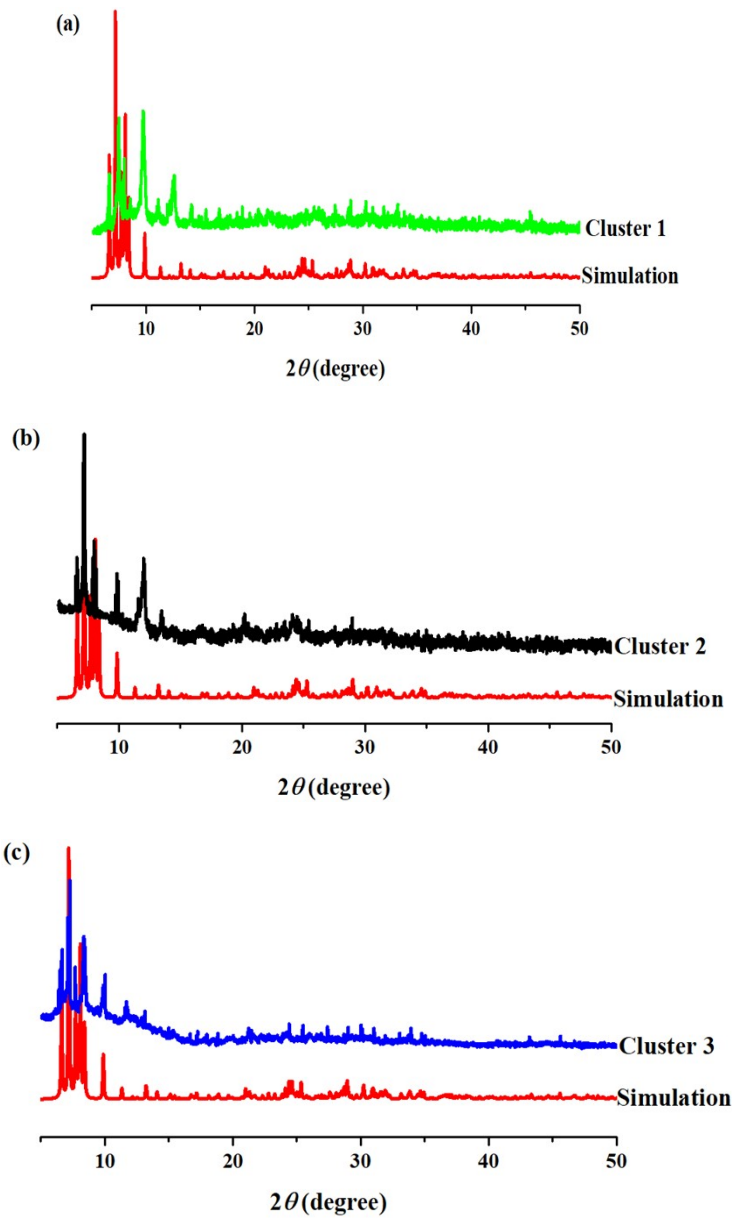


Fig. S7 PXRD patterns for clusters 1-3.

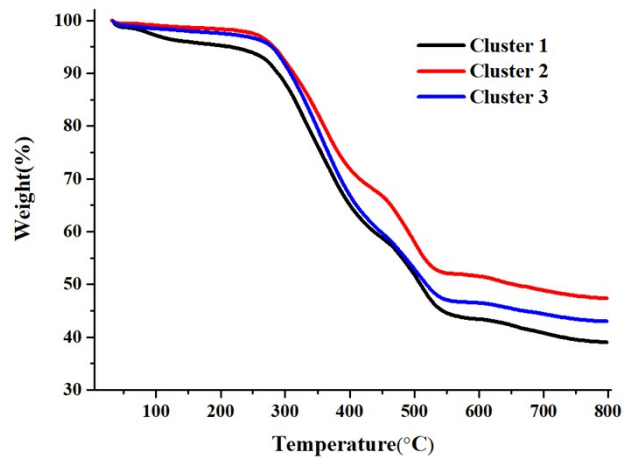


Fig. S8 The TGA curves of clusters 1-3.

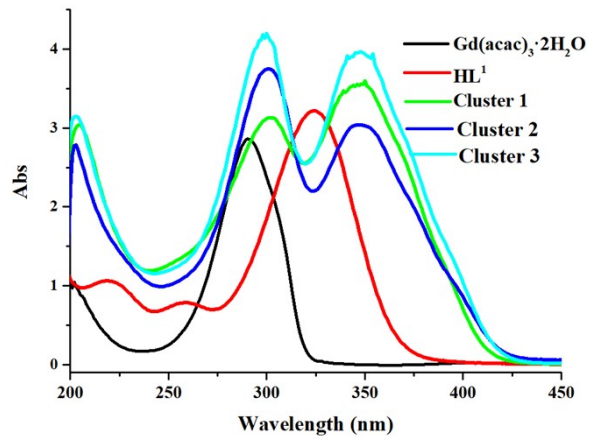


Fig. S9 The UV-vis spectra of clusters **1-3**, Gd(acac)₃ · 2H₂O and the HL ligand were performed at room temperature in ethanol solution.

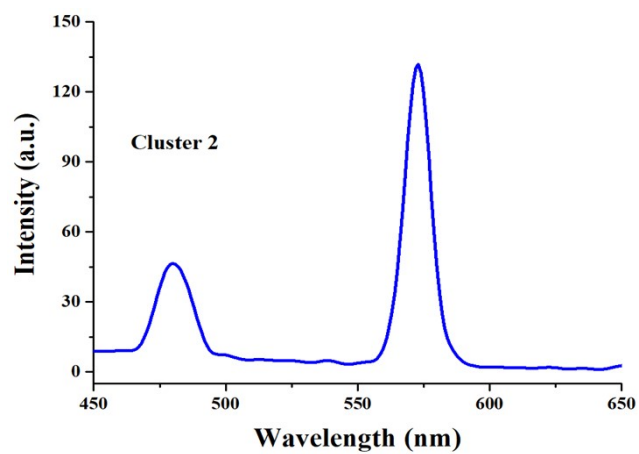


Fig. S10 Fluorescence emission spectra of cluster **2** in DMF at room temperature.

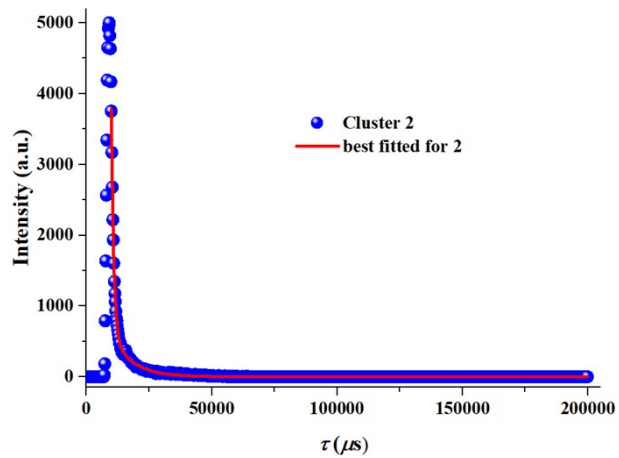


Fig. S11 The fluorescence emission lifetime of cluster **2** in DMF.

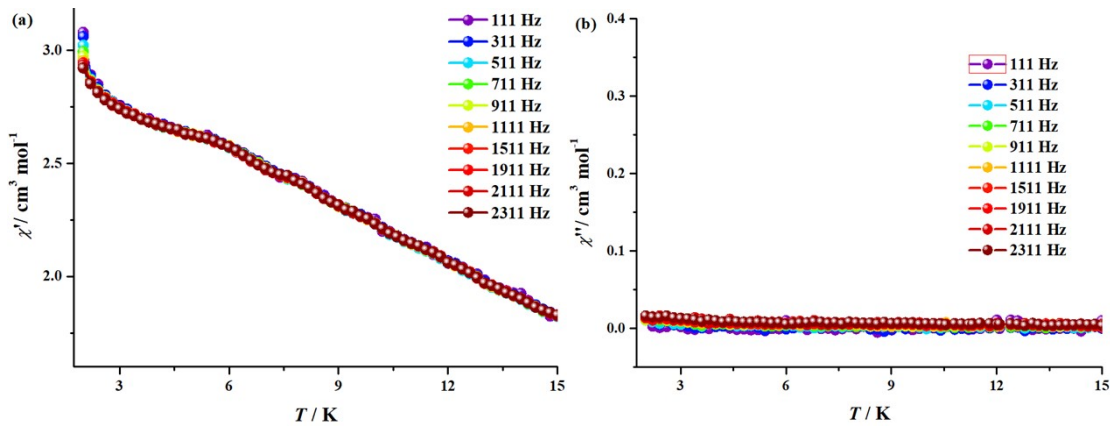


Fig. S12 Temperature dependence of the in-phase (left) and out-of-phase (right) components of the ac magnetic susceptibility for **3** in zero dc field with an oscillation of 3.0 Oe.

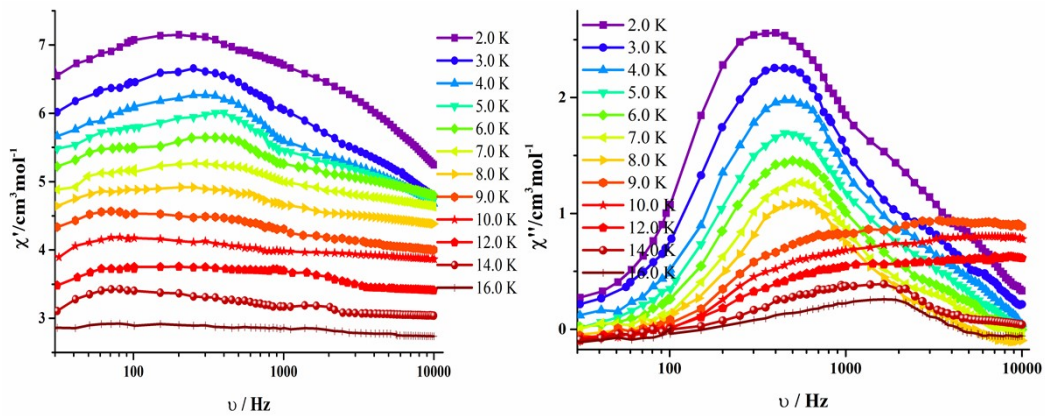


Fig. S13 Frequency dependence of χ' and χ'' for **2** at 2.0–16.0 K under zero dc field.

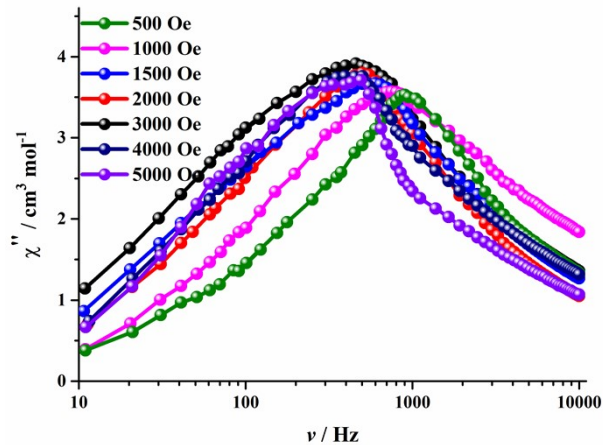


Fig. S14 The frequency dependency of the χ'' ac susceptibility was measured on **2** under the applied field from 500 to 5000 Oe at 2.0 K.

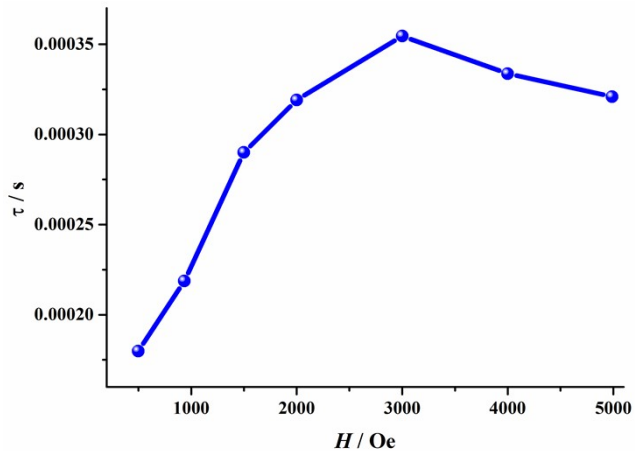


Fig. S15 The τ versus H plot for **2** under different applied dc field.

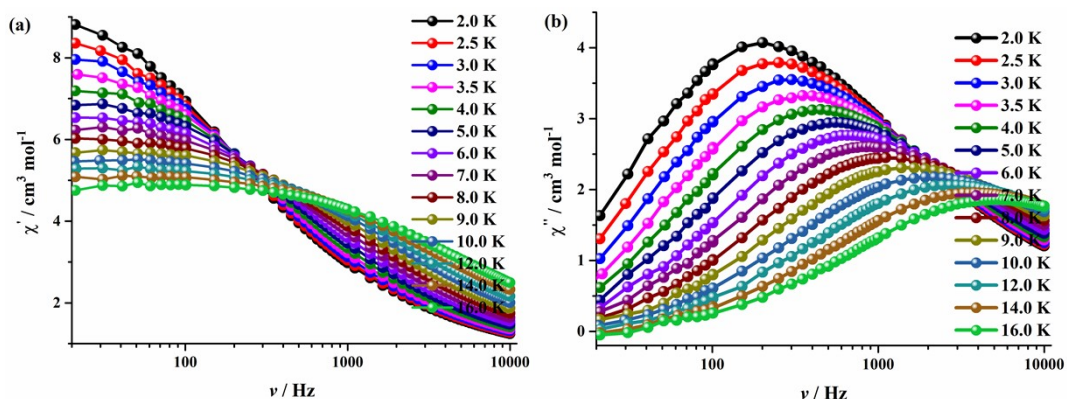


Fig. S16 Frequency dependence of χ' and χ'' for **2** at 2.0–16.0 K under the optimum field ($H_{dc} = 3000$ Oe).

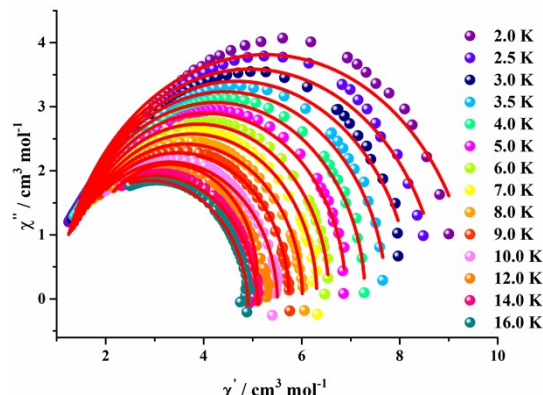


Fig. S17 Cole–Cole plots for **2** measured under the optimum field ($H_{dc} = 3000$ Oe). The solid red lines are the best fit to the experimental data, obtained with the generalized Debye model with $\alpha = 0.08\text{--}0.51$.

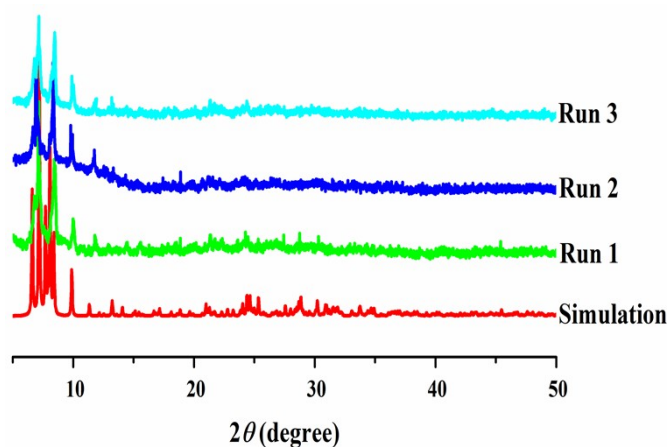


Fig. S18 PXRD pattern of **1** and the recycled catalyst after reactions.

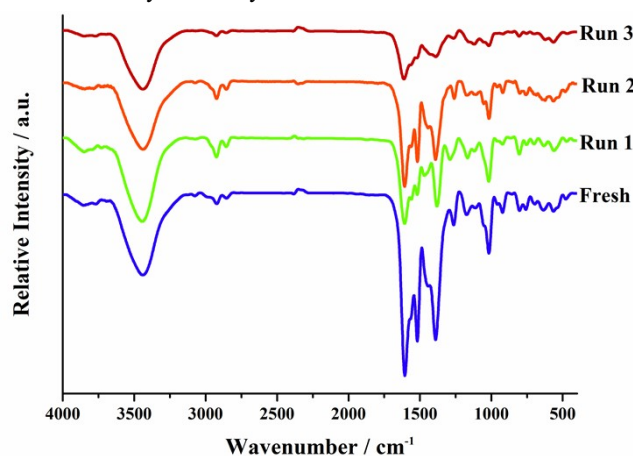
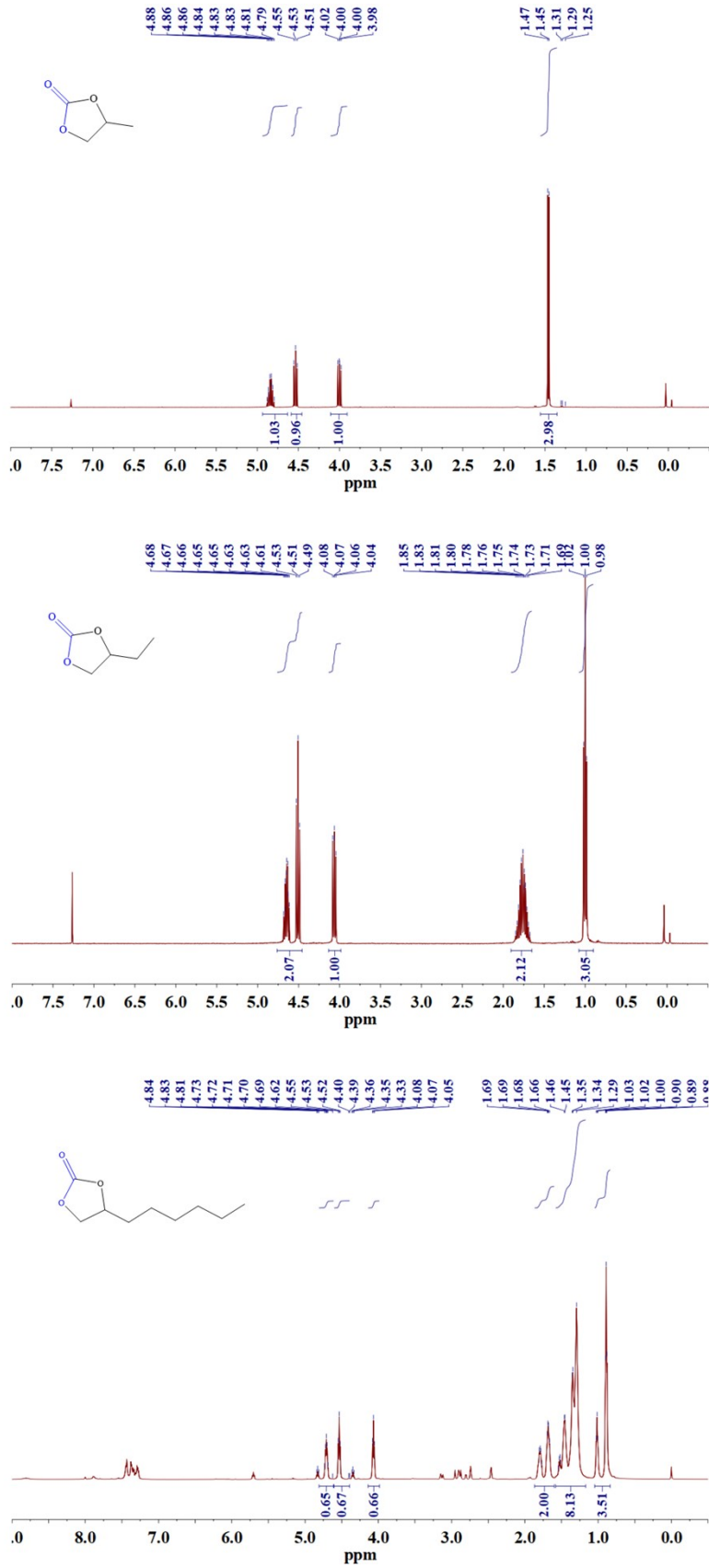


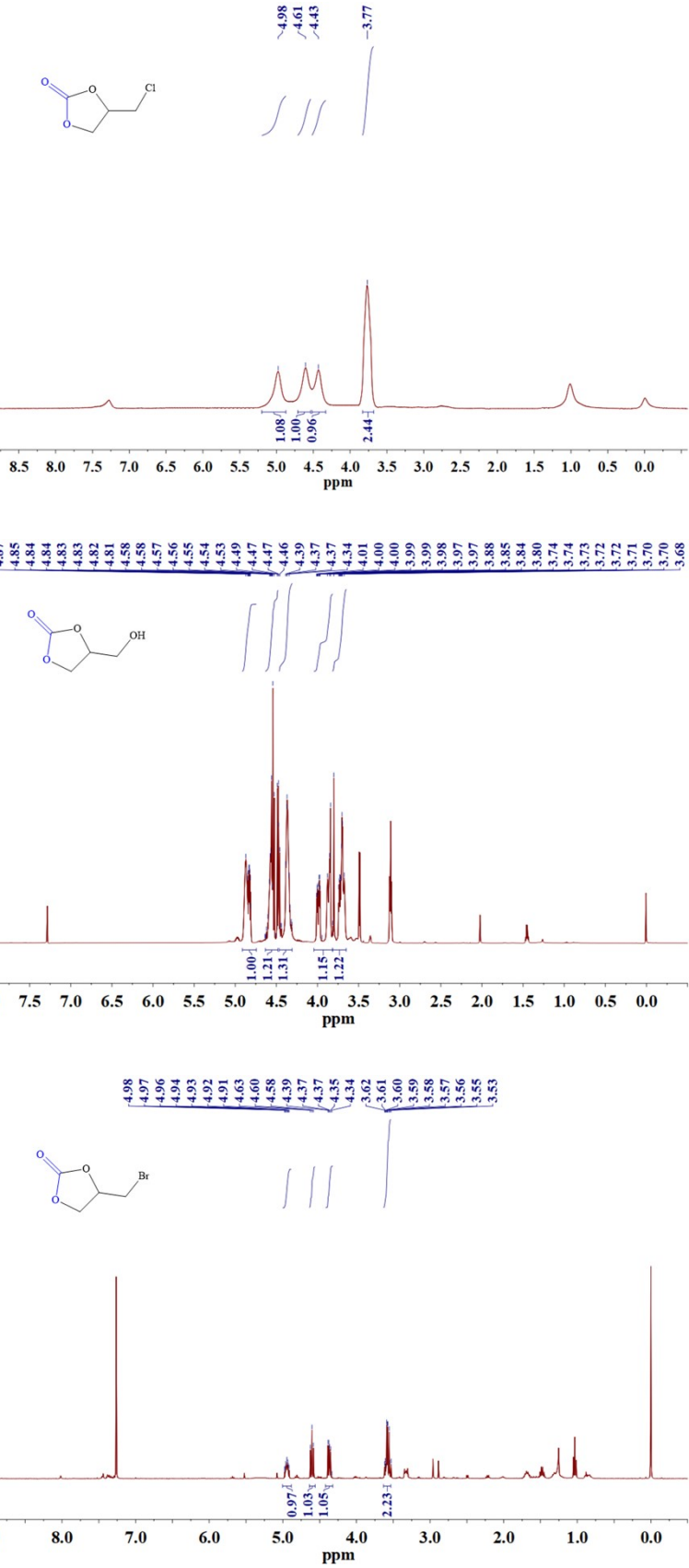
Fig. S19 IR spectra of cluster **1** and after recycled reaction.

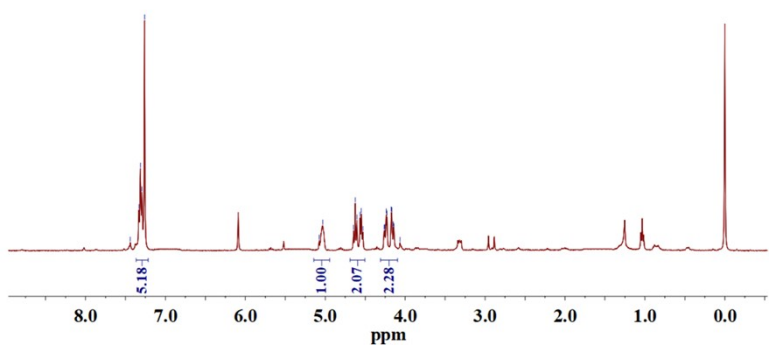
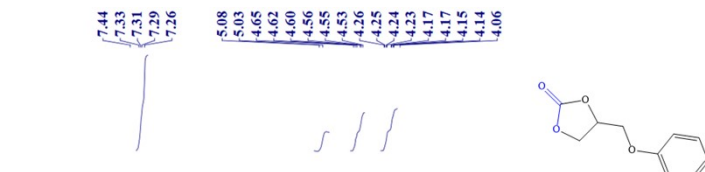
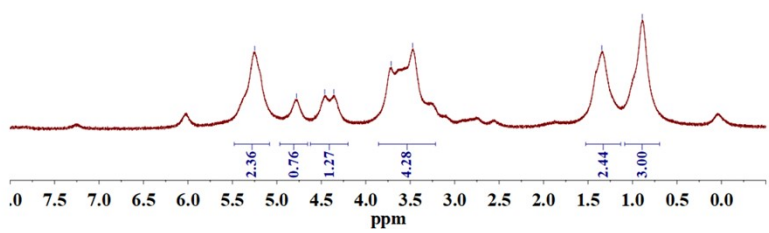
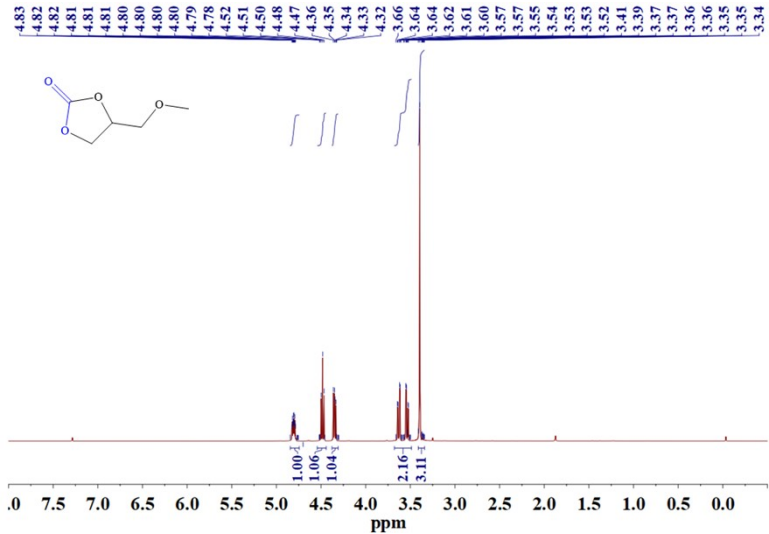
Table S5 The ICP results of cluster **1** after recycling (filter liquor).

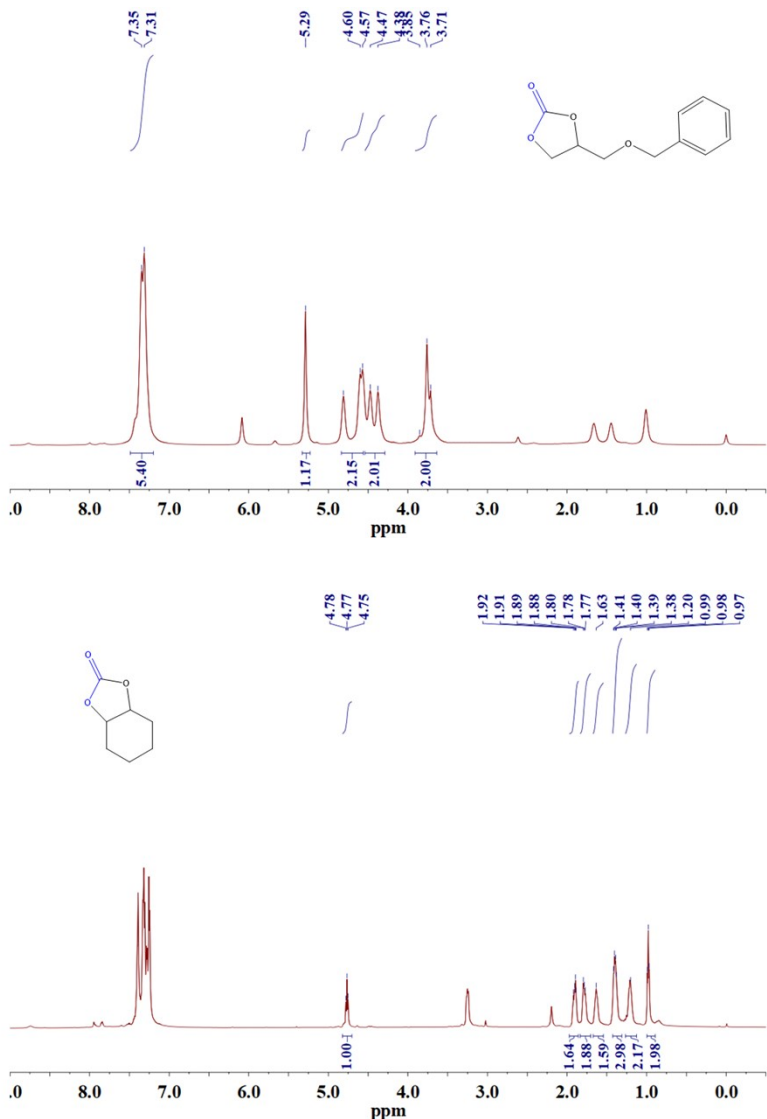
Cluster 1	Gd ^(III)
Cluster 1 after catalytic recycling (filter liquor)	0.41 %

¹H NMR spectral for various cyclic carbonates









Notes and references

- W. M. Wang, T. T. Zhang, D. Wang and J. Z. Cui, Structures and magnetic properties of novel Ln(III)-based pentanuclear clusters: magnetic refrigeration and single-molecule magnet behavior, *New J. Chem.*, 2020, **44**, 19351-19359.
- S. Katagiri, Y. Tsukahara, Y. Hasegawa and Y. Wada, Energy-transfer mechanism in photoluminescent terbium(III) complexes causing their temperature-dependence, *Bull. Chem. Soc. Jpn.*, 2007, **80**, 1492-1503.